Modeling the effects of post-anthesis heat stress on rice phenology

ARTICLE *in* FIELD CROPS RESEARCH · FEBRUARY 2015

Impact Factor: 2.61 · DOI: 10.1016/j.fcr.2015.02.023

7 AUTHORS, INCLUDING:

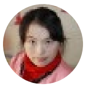

Peihua Shi
Nanjing Agricultural University
3 PUBLICATIONS **2** CITATIONS
SEE PROFILE

Leilei Liu
Nanjing Agricultural University
9 PUBLICATIONS **39** CITATIONS
SEE PROFILE

Yan Zhu
Nanjing Agricultural University
115 PUBLICATIONS **434** CITATIONS
SEE PROFILE

Field Crops Research 177 (2015) 26–36

Contents lists available at ScienceDirect

Field Crops Research

journal homepage: www.elsevier.com/locate/fcr

Modeling the effects of post-anthesis heat stress on rice phenology

Peihua Shi, Liang Tang, Chunbo Lin, Leilei Liu, Huanhuan Wang, Weixing Cao, Yan Zhu*

National Engineering and Technology Center for Information Agriculture (NETCIA), Jiangsu Key Laboratory for Information Agriculture, Jiangsu Collaborative Innovation Center for Modern Crop Production, Nanjing Agricultural University, Nanjing, Jiangsu 210095, P.R. China

ARTICLE INFO

Article history:
Received 12 April 2014
Received in revised form 8 August 2014
Accepted 24 February 2015

Keywords:
Climate change
Heat stress
Crop model
Phenology
Rice

ABSTRACT

Heat stress significantly accelerates senescence process during reproductive phase in rice, but the effects of heat stress are not yet well simulated by most of the existing crop models. Three-year experiments under different temperature levels and temperature durations at anthesis and 12 days after anthesis were carried out in phytotron using two japonica cultivars. Significant positive correlations were observed between the shortened grain growing days from anthesis to maturity (GD_{AM}) and heat degree-days (HDD). The impact of post-anthesis heat stress on rice phenology was quantified by adding thermal effectiveness of heat stress to the original RiceGrow model. Performance of the improved model was tested with phenological data from different cultivars under post-anthesis heat stress of phytotron environments and field conditions. Validation results showed that root mean square error (RMSE), mean bias error (MBE) and variance of the distribution of differences (S_d^2) for the prediction of GD_{AM}, decreased from 4.60 d, 2.65 d and 7.80 in the original model to 1.58 d, −0.16 d and 2.40 in the improved model, respectively, under post-anthesis heat stress conditions. The determination coefficient (R^2) and index of agreement (IA) between simulated and observed GD_{AM}, increased from 68.5% and 0.71 in the original model to 93.5% and 0.92 in the improved model under post-anthesis heat stress conditions, respectively. Overall, the improved model gave better predictions of GD_{AM} in different rice cultivars under different post-anthesis heat stress environments. Our study highlights the necessity of accurately simulating the heat stress effects on phenological processes in rice to forecast crop production for ensuring food security under climate change reliably.

1. Introduction

Extreme high temperature events are becoming more frequent due to the increasing temperature and climatic variability (Lloret et al., 2012; Lobell et al., 2011; Schlenker and Roberts, 2009). Several studies reported that warming temperature due to climate change will shift phenology forward for field crops (Chmielewski et al., 2004; Liu et al., 2012; Tao et al., 2006), but few studies mentioned the impacts of heat stress on crop phenology. High temperature during reproductive stage shortens grain filling duration, reduces the contribution of stored assimilates to grains and eventually leads to lower grain weight and yield in rice (Kim et al., 2011; Prasad et al., 2006). Yield loss that caused by the shortened developmental process due to heat stress has posed a great risk to crop production (Moriondo et al., 2011; Prasad et al., 2008).

The process-based crop model, which can simulate the interaction of genotypes, environmental factors and management practices, has become an effective tool to estimate crop productivity under climate change. However, most of the previous crop models were developed under stable climatic conditions (Angulo et al., 2013; Boote et al., 1996). Recently, the shortcomings and uncertainties of crop model were gradually found under extreme climatic conditions (Lobell et al., 2012; Moriondo et al., 2011; Zhang and Tao, 2013). For many process-based crop models, simulations of some crop growth processes such as dry matter partitioning and leaf area dynamic are directly dependent on crop phenological development (Cao and Moss, 1997; White et al., 1997). Therefore, the simulation of phenological process is the basis for the accurate prediction of crop productivity.

Temperature is the main factor that affects the whole crop developmental process. Phenology simulation is based on the thermal time accumulation in various crop models such as CERES v3.x (Xue et al., 2004), ORYZA2000 (Bouman, 2001) and APSIM (Zhang et al., 2004). In previous simulation studies, these crop models were driven by an implicit assumption that the thermal time accumulation for the entire growing season would remain constant under various climatic conditions. Zhang et al. (2008) found that the thermal time accumulation in rice crop for the entire

---

* Corresponding author. Tel.: +86 25 84396598; fax: +86 25 84396672.
E-mail address: yanzhu@njau.edu.cn (Y. Zhu).

http://dx.doi.org/10.1016/j.fcr.2015.02.023
0378-4290/

growing season was not constant, and crop models based on constant thermal time accumulation significantly underestimate the observed phenological process under climate warming conditions. Phenology models differed in their response to the temperature above the optimal value, due to the difference in temperature response curves and temperature variables. The assumption of a rapid decrease in development rate above the optimal temperature in most models could lead to poor predictions and systematic errors (Van Oort et al., 2011; Sadras and Monzon, 2006; Zhang and Tao, 2013). In recent years, much work was addressed to the improvement of phenology model under high temperature during the main development stages despite of limited understanding of physiological mechanism in crops. The newly released version of CERES-Wheat 4.0 employed a trapezoidal model to simulate the response of development rate to temperature instead of a bilinear model in the older version, and the development rate was maintained the maximal value from 30 °C to 50 °C during post-anthesis stage (McMaster et al., 2008; White and Hoogenboom, 2010). Afterwards, White et al. (2011) revised the cardinal temperatures for spring wheat using phenological data from a series of sowing dates trials, and identified that the optimal temperature after anthesis is between 34 °C and 50 °C in the version of CERES-Wheat 4.5. Although similar simulation biases of phenology models were found in rice crop under climate warming conditions (Van Oort et al., 2011; Wassmann et al., 2009; Zhang and Tao, 2013), the necessary improvements were hardly reported due to the insufficient available phenological data and limited understanding of phenological responses to high temperatures in rice crop.

The main objectives of this study are: (1) to determine the impact of post-anthesis heat stress on phenological development in rice based on the experimental data from different high-temperature treatments in phytotron in 2011–2013, (2) to improve the model algorithms for the simulation of rice phenology under post-anthesis heat stress based on the original model RiceGrow, (3) to evaluate and compare the performances of the original model and newly improved model with independent experimental dataset under post-anthesis heat stress of phytotron environments and field conditions.

2. Materials and methods

2.1. Introduction of the original RiceGrow model

The original RiceGrow model is a process-based model, which can simulate phenology, morphology and organ formation, photosynthesis, biomass accumulation and partitioning, water and nutrient dynamics, grain yield and quality formation of various genotypes in response to environmental factors and management practices (Liu et al., 2012; Tang et al., 2009). The physiological development time (PDT) was used to quantify the effects of temperature and photoperiod on phenological development in the original model (Cao and Moss, 1997; Meng et al., 2003). The life cycle of rice crop is divided into four developmental phases: basic vegetative phase (BVP, from seedling emergence to the initiation of photoperiod-sensitivity), photoperiod sensitive phase (PSP, from the initiation of photoperiod-sensitive phase to the initiation of panicle), panicle formation phase (PFP, from the initiation of panicle to 50% flowering), and grain-filling phase (GFP, from 50% flowering to physiological maturity). The corresponding PDT of the above four phases are 0–8, 8–18, 18–32 and 32–57, respectively. There are four genetic parameters in the original model that affect phenological development. They are thermal sensitivity (TS), intrinsic earliness (IE), photoperiod sensitivity (PS), and basic filling factor (BFF). TS reflects the temperature sensitivity of whole growth period in different cultivars, with a range of 2.0–6.0. IE affects the growth duration from emergence to the beginning of photoperiod-sensitive phase and has values between 0 and 1.0, with 1.0 representing the shortest duration for cultivar growth during that stage. PS determines the photoperiod sensitivity for different cultivars from the initiation of photoperiod-sensitive phase to the initiation of panicle, which ranges from 0 to 0.2, with higher values in more photoperiod-sensitive cultivars. BFF affects the growth duration between anthesis and physiological maturity and ranges from 0 to 1.0, with 1.0 for cultivars having the shortest growth duration between anthesis and physiological maturity (Liu et al., 2012).

The PDT is the sum of daily physiological effectiveness (DPE_i). DPE_i is determined by the interaction of daily thermal effectiveness (DTE_i) and daily relative photoperiod effectiveness (RPE_i), or intrinsic earliness (IE) or basic filling factor (BFF), calculated as Eq. (1):

$$\mathrm{DPE}_i = \begin{cases} \mathrm{DTE}_i \times \mathrm{IE} & 0 \le \mathrm{PDT} \le 8 \\ \mathrm{DTE}_i \times \mathrm{RPE}_i & 8 \le \mathrm{PDT} \le 18 \\ \mathrm{DTE}_i & 18 \le \mathrm{PDT} \le 32 \\ \mathrm{DTE}_i \times \mathrm{BFF} & 32 \le \mathrm{PDT} \le 57 \end{cases} \tag{1}$$

A quadratic equation is used to describe RPE_i in RiceGrow model, as Eq. (2):

$$\mathrm{RPE}_i = \begin{cases} 1 & P_i \le P_o \\ 1 - \mathrm{PS} \times (P_i - P_o)^2 & P_o < P_i \le P_c \\ 0 & P_i > P_c \end{cases} \tag{2}$$

where PS reflects the photoperiod sensitivity among different cultivars; P_i is the observed day length on day i; P_o is the optimum day length for heading; P_c is the critical day length for heading, calculated as Eq. (3):

$$P_\mathrm{c} = P_\mathrm{o} + \left(\frac{1}{\mathrm{PS}}\right)^{0.5} \tag{3}$$

The variable DTE_i is obtained by the average value of hourly relative thermal effectiveness (RTE_j), calculated as Eq. (4):

$$\mathrm{DTE}_i = \frac{1}{24} \times \sum_{1}^{24} \mathrm{RTE}_j \tag{4}$$

RTE_j, which reflects the effect of hourly temperature on development rate of rice, ranges between 0 and 1. A beta function is used to quantify the relationship between RTE_j and temperature in RiceGrow model, calculated as Eq. (5):

$$\mathrm{RTE}_j = \begin{cases} \left[\left(\dfrac{T_j - T_\mathrm{b}}{T_\mathrm{o} - T_\mathrm{b}}\right)\left(\dfrac{T_\mathrm{c} - T_j}{T_\mathrm{c} - T_\mathrm{o}}\right)^{(T_\mathrm{c} - T_\mathrm{o})/(T_\mathrm{o} - T_\mathrm{b})}\right]^{\mathrm{TS}} & T_j < T_\mathrm{o} \\ 1 & T_j \ge T_\mathrm{o} \end{cases} \quad (j = 1, 2, \ldots, 24) \tag{5}$$

where j is the hour of the day; T_b, T_o and T_c are the base temperature, optimum temperature and critical high temperature, with the values of 8 °C, 30 °C and 42 °C, respectively (Liu et al., 2013). T_j is the hourly temperature calculated from daily minimum temperature (T_min) and daily maximum temperature (T_max), as Eq. (6):

$$T_j = \frac{T_\mathrm{max} + T_\mathrm{min}}{2} + \frac{T_\mathrm{max} - T_\mathrm{min}}{2} \times \cos\left[\frac{\pi}{12} \times (j - 14)\right] \quad (j = 1, 2, \ldots, 24) \tag{6}$$

Table 1
Basic information of experiments in phytotron and field conditions.

Experiment environment	Cultivar	Cropping season	Type and maturity	Eco-site	Latitude, longitude	Years for calibration	Years for validation
Phytotron	Nanjing41	SR	Japonica and late	Nanjing	32°11′ N, 118°28′ E	2011–2012	2013
	Wuxiangjing14	SR	Japonica and early	Nanjing	32°11′ N, 118°28′ E	2011–2012	2013
Field	Wuyujing3	SR	Japonica and late	Yixing	31°20′ N, 119°49′ E	1992–1997	2000, 2003, 2005
				Zhenjiang	32°11′ N, 119°27′ E	1991–1994	–
	8304	SR	Japonica and mid	Chuzhou	32°18′ N, 118°18′ E	1992–1996	1986–1987, 1991
				Hefei	31°52′ N, 117°14′ E	1992–1996	–
	Shanyou63	SR	Indica and late	Zhongxiang	31°10′ N, 112°34′ E	1987–1990	–
				Wuhan	30°37′ N, 114°08′ E	1990–1992	1993, 1995
				Suizhou	31°43′ N, 113°23′ E	1990–1992	1995
	Xiang’aizao9	DER	Indica and late	Changsha	28°12′ N, 113°05′ E	1981–1983	1984, 1986
				Hengyang	26°53′ N, 112°30′ E	1981–1984	–
				Lingling	26°25′ N, 111°34′ E	1981–1983	1984–1985
	Zhefu802	DER	Indica and early	Changsha	28°12′ N, 113°05′ E	1987–1991	–
				Changde	29°03′ N, 111°41′ E	1987–1991	1992, 1994–1995
	YouI402	DER	Indica and early	Zhangshu	28°04′ N, 115°33′ E	2000–2004	2005, 2008
				Guangfeng	28°42′ N, 116°21′ E	2000, 2003–2006	2007, 2009
	73-07	DER	Indica and mid	Guangfeng	28°42′ N, 116°21′ E	1987–1990	1991, 1994
				Taihe	26°48′ N, 114°55′ E	1992–1994	–
				Ruichang	29°41′ N, 115°40′ E	1986–1988	1995, 1998
	Guanglu’ai4	DER	Indica and late	Jiaxing	30°47′ N, 120°44′ E	1981–1984	–
				Quzhou	28°58′ N, 118°52′ E	1981–1983	1984, 1987
				Ninghai	29°18′ N, 121°26′ E	1981–1983	1984–1985

SR and DER indicate single-season rice and double-season early rice, respectively.

2.2. *Modeling the effects of post-anthesis heat stress on rice phenology*

The phenological process from anthesis to maturity was mainly determined by temperature. Post-anthesis phenological development under high temperatures would include the normal temperature effects which resulted in the normal senescence and the heat stress effects which accelerated the senescence process, as described by Lobell et al. (2012, 2013). Thus the daily thermal effectiveness (DTE_i) for rice development from anthesis to maturity should be composed by daily thermal effectiveness of normal temperature (DTENT_i) and daily thermal effectiveness of heat stress (DTEHS_i) that accelerated phenological process, calculated as Eq. (7):

$$\mathrm{DTE}_i = \mathrm{DTENT}_i + \mathrm{DTEHS}_i \tag{7}$$

where the calculation of DTENT_i is same as that of DTE_i in the original model (Eqs. (4)–(6)), and DTEHS_i is calculated as Eq. (8):

$$\mathrm{DTEHS}_i = \frac{\sum_{1}^{d_i}\mathrm{HD}_i}{\beta \times \mathrm{GDD}_{\mathrm{AM}}} \tag{8}$$

where HD_i is the daily heat degree-days (°C), calculated by hourly temperature as Eq. (9); β is the heat sensitivity factor in rice; $\mathrm{GDD}_{\mathrm{AM}}$ is the requirement of growing degree-days (GDD) from anthesis to maturity, set as 620 °C d in japonica rice and 520 °C d in indica rice by comprehensively analyzing the experimental data from phytotron and field conditions with different cultivars at different ecosites during different years (Table 1).

$$\mathrm{HD}_i = \frac{1}{24} \times \sum_{j=1}^{24}\mathrm{HHD}_j \tag{9}$$

$$\mathrm{HHD}_j = \begin{cases} 0 & T_j \le T_h \\ T_j - T_h & T_j > T_h \end{cases} \quad (j = 1, 2, \ldots, 24) \tag{10}$$

where HHD_j indicates the hourly heat degree-days; T_j is the hourly temperature as calculated by Eq. (6); T_{h} represents the threshold temperature of heat stress, and is set as 35 °C in the improved Rice-Grow model by comprehensively analyzing the published results (Luo, 2011; Sun and Huang, 2011; Teixeira et al., 2013; Wassmann et al., 2009) and our experiment results in phytotron.

Therefore, the simulation of DTE_i in the original model (Eqs. (4)–(6)) was instead with Eqs. (7)–(11) for an improved model, which can better predict the thermal effectiveness of heat stress.

2.3. *Data sources*

2.3.1. *The temperature-controlled experiments in phytotron*

In order to investigate the influence of post-anthesis heat stress on rice phenological development, temperature-controlled experiments were conducted during 2011–2013 in phytotron at Nanjing Agricultural University, Nanjing, China (32.04° N, 118.78°E). Two japonica cultivars ‘Nanjing41’ (heat-sensitive) and ‘Wuxiangjing14’ (moderate heat-tolerance) were used in each experiment. Seedlings were raised for about 22 days (d) in a nearby paddy field, and then transplanted to 600 plastic pots (with an inside diameter of 28.8 cm and a height of 35.6 cm) filled with 20 kg air-dried paddy soil. Plants were grown in outdoor with a fertilization rate of 3.0 g N, 2.0 g P_2O_5, and 1.5 g K_2O per pot. The pots with plants of 50% flowering on the same day were selected to implement the treatments of different temperature levels and temperature durations. At anthesis and 12 days after anthesis (in the early stage of grain filling), pots were transferred to four phytotron rooms severally with the maximum/minimum temperature gradients of 32/22 °C (T1), 35/25 °C (T2), 38/28 °C (T3) and 41/31 °C (T4) under natural daylight conditions. Durations of high-temperature under different high-temperature levels were designed as 2 d (D1), 4 d (D2) and 6 d (D3). The information of different high-temperature treatments was summarized in Table 2.

The phytotron rooms measured 4.4 m × 4.2 m × 2.8 m (L × W × H), covering with high transparent glasses (75% optical transparency). Each chamber was equipped with an air conditioner capable of maintaining constant temperatures. Daily temperature variation in phytotron was controlled to simulate the diurnal change pattern of temperature in ambient environment, and temperature fluctuations at each given time were within 1 °C (Fig. 1a). The relative humidity (RH) was maintained to 70 ± 5% by the control of a humidity regulator (Fig. 1b). There were one inlet and one outlet fan installed in the front and back frames,

Table 2
Treatment information of experiments in phytotron from 2011 to 2013.

Year	Cultivar	Anthesis date (Month-date)	Temperature level and duration
2011	Nanjing41	8–19	T1 and D2 T2 and D1, D2, D3
	Wuxiangjing14	8–27	T3 and D2 T4 and D1, D2, D3
2012	Nanjing41	8–20	T1 and D2
	Wuxiangjing14	8–25	T2 and D2
2013	Nanjing41	8–21	T3 and D1, D2, D3
	Wuxiangjing14	8–27	T4 and D1, D2, D3

T1, T2, T3 and T4 indicate the temperature levels (T_{max}/T_{min}) of 32/22 °C, 35/25 °C, 38/28 °C and 41/31 °C, respectively; D1, D2 and D3 indicate the durations of 2 days (d), 4 d and 6 d under different temperature levels, respectively. Each year, the treatment started from the anthesis and 12 days after anthesis (12DAA), respectively.

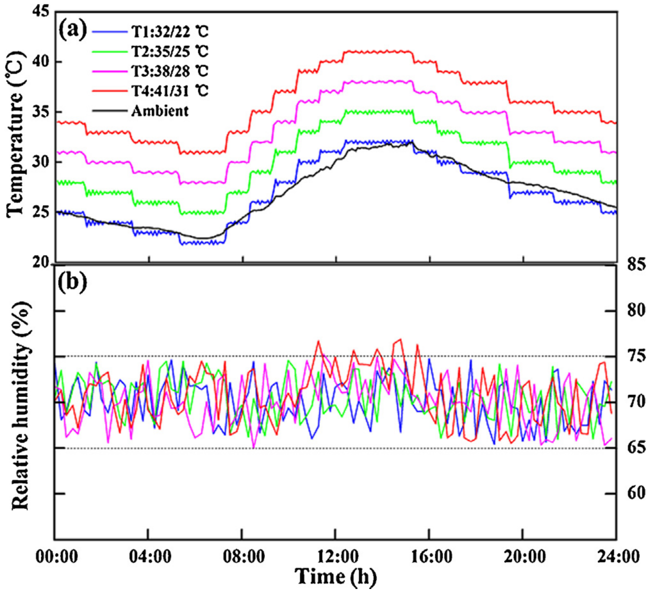

Fig. 1. The daily variation of (a) air temperature and (b) relative humidity in four phytotron rooms (data were obtained on 4th September 2011).

respectively, to minimize the differences of CO_2 concentration between the chamber and the ambient environment by constant but mild air exchange. The inner and outer pots in the same chamber were exchanged every day at 17:00 in case of uneven distribution of light. Water depth in the pots was maintained at about 5 cm throughout the treatment period. Temperature and RH in phytotron were measured once every 5 min using HOBO data loggers (Onset Computer Corp., Bourne, MA, USA) with the standalone sensors above the canopy.

2.3.2. *The field experiments with post-anthesis heat stress*

Observed phenological data from 108 field experiments was used for model calibration and validation, which were operated by the Chinese Meteorological Administration (CMA). The 108 field experiments distributed at 18 ecosites in the main rice planting regions of south China (26°25′–32°18′ N, 111°34′ E–121°26′ E) between 1981 and 2009, with three cultivars from single-season rice regions and five cultivars from double-season rice regions (Table 1). In order to obtain more accurate cultivar parameters to better reflect genetic characters, the cultivars were selected with different ecotypes and maturity characteristics. Moreover, phenological data of each cultivar was chosen from different ecosites to eliminate the locational properties of genetic parameters. In the double-season rice region, only phenological data during the early rice season were used in this study, because normally no post-anthesis heat stress was observed during the late rice season.

2.3.3. *The observed dataset from phytotron and field conditions*

The dates of sowing, transplanting, anthesis and physiological maturity under different treatments in each experiment were measured and recorded in both phytotron and filed environments. Anthesis was defined as the date of 50% plants with florets opening at the middle-upper position of the panicles, and measured by regular observation on the number of flowering panicles. Maturity, i.e. physiological maturity, was specified as the date when grains reach maximum dry weight during development (Shaw and Loomis, 1950). At anthesis, 450 uniform panicles were tagged for each temperature treatment. A total of 30 tagged panicles were sampled from each treatment at 0, 6, 12, 18, 24, 30, 34, 37, 39, 41, 43, 45, 47, 49, 51 days after anthesis. Grain seeds were gently threshed by hand and unfilled grains were removed (Zhu et al., 1988). The filled grains were dried to constant weight at 70 °C, and three random samples of 1000 grains were weighted. A cubic polynomial equation was used to fit the dynamic change of grain weight by least square regression as proposed by Jones et al. (1979). Grain-filling rates at any given time were gained by taking the derivation of the cubic polynomial equation:

$$\frac{dy}{dx} = 3a_1x^2 + 2a_2x + a_3 \tag{11}$$

where y indicates the grain weight; x indicates day after anthesis; a_1, a_2 and a_3 are the coefficients estimated by fitting the cubic polynomial equation. The date of physiological maturity for each treatment was determined by setting dy/dx = 0, and solving for the independent time variable (Hanft and Wych, 1982).

Under field conditions, the daily weather data (maximum temperature, minimum temperature, sunshine hour and precipitation) were obtained from the China Meteorological Data Sharing Service System (http://cdc.cma.gov.cn). In phytotron conditions, the daily weather data before and after treatment of heat stress were recorded by Dynamet-1K (Dynamet Inc., USA) at the experiment site, while that during the treatment of heat stress under phytotron conditions was recorded by using HOBO data loggers (Onset Computer Corp., Bourne, MA, USA) with the standalone sensors above the canopy, respectively.

The experiment data observed from phytotron environments after temperature treatments were used to investigate the effect of post-anthesis heat stress on rice phenology. Both of experiment data from field and phytotron environments were divided into two independent groups for model calibration and validation, respectively. More details of experiment data utilization can be found in Table 1 and Fig. S1.

Model calibration was carried out with phenological data from different temperature environments (including normal temperature and post-anthesis heat stress environments) of two cultivars in phytotron in 2011–2012 and of eight cultivars under field conditions at different ecosites during different years (each cultivar with 10 years data from 2 to 3 different ecosites).

In order to accurately reflect the effects of model improvement, the phenological data from phytotron environments in 2013 and that from field conditions with post-anthesis heat stress records at different ecosites were selected for model validation. In addition, each cultivar in field experiments has 3- or 4-year phenological data records under different post-anthesis heat degree-days (HDD, range from 0.61 to 24.56 °C d).

2.4. Analysis methods

2.4.1. The impact of post-anthesis heat stress on rice phenology

The differences between the grain growing days from anthesis to maturity (GD_{AM}) under post-anthesis high temperatures (T2, T3, T4) and that under suitable temperature (T1) were calculated to indicate the shortened development time after anthesis under different post-anthesis high-temperature treatments. Then a simple linear regression was used to fit the relationship between GD_{AM} and HDD to detect the effects of post-anthesis heat stress on rice phenology.

2.4.2. Model calibration

The code of phenology module in the original and improved models was both rewritten in R (R Core Team, 2014). The genetic parameters were estimated by Nelder–Mead simplex method (Nelder and Mead, 1965) with optim() function of R. This method was commonly used for parameter estimation in several studies (Casa et al., 2012; Jégo et al., 2012; Wallach, 2011). Since the model improvement was about phenological development from anthesis to maturity, RiceGrow model was set to start simulation at the observed anthesis dates. Hence, genetic parameters that determined the post-anthesis developmental process were calibrated in RiceGrow model, i.e. TS and BFF for the original model, and TS, BFF and β for the improved model. The genetic parameters in the original and improved models were calibrated to best match the estimated phenological dates with observed values, respectively.

2.4.3. Sensitivity analysis of phenological development to post-anthesis heat stress

Sensitivity analysis of phenological development to simulated post-anthesis heat stress was performed on the improved RiceGrow model. In the simulated post-anthesis heat stress, two high-temperature levels (T_{max}/T_{min}: 38/28 °C and 41/31 °C) with three high-temperature durations (2 d, 4 d and 6 d) were applied starting from each available days after anthesis. In addition, the fixed daily temperature with T_{max}/T_{min} of 28/18 °C was used during the days after anthesis without heat events. Other input dataset that required in RiceGrow model were from the observed dataset of Wuxiangjing14 in our phytotron experiment in 2011. The variation of predicted GD_{AM} generally represented the changes in the sensitivity of phenological development to post-anthesis heat stress.

2.4.4. Model validation

To assess the performance of original and improved models, four statistical indices were calculated between the estimated and observed values as reported by Palosuo et al. (2011). Root mean square error (RMSE) provides a measure of the relative average difference between model estimates and observed values. Mean bias error (MBE) is an index to inform whether the models under- or overestimated the measurements, i.e. the direction and magnitude of bias. Variance of the distribution of differences (S_d^2) is used to quantify the error variability. Index of agreement (IA) is a general index of modeling efficiency. The above four statistical indices measure the mean residuals of the model from different aspects and the corresponding formula can be found in Rötter et al. (2012). In addition, the determination coefficient (R^2) between simulated and observed values is calculated although it does not take into account model bias, which is central when estimating model performance (Palosuo et al., 2011).

Correlations between the post-anthesis HDD and the prediction error (the difference between observed and predicted values) of GD_{AM} in the original model and improved model were both analyzed, to confirm the effects of model improvements.

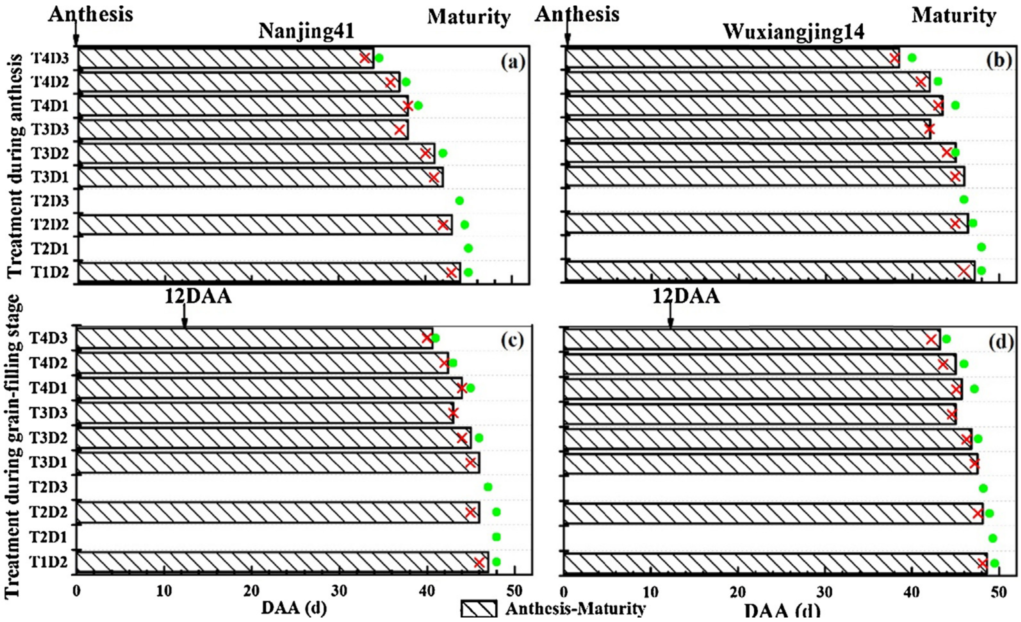

Fig. 2. Developmental processes of (a and c) Nanjing41 and (b and d) Wuxiangjing14 under different temperature treatments at anthesis and 12 days after anthesis (12DAA). Horizontal bar with backslash indicates observed maturity for the two cultivars in 2012, while green solid dot and red cross indicate the observed maturity in 2011 and 2013, respectively. Black arrow indicates the starting time of temperature treatment. (For interpretation of the references to color in this figure legend, the reader is referred to the web version of this article.)

3. Results

3.1. *The impact of post-anthesis heat stress on phenological processes*

Post-anthesis development processes for Nanjing41 and Wuxiangjing14 under different temperature treatments were shown in Fig. 2. Under the treatments at anthesis, the average growing days from anthesis to maturity (GD_{AM}) under T2D2, T3D2, T4D2 shortened 1.0 d, 3.0 d, 7.3 d in Nanjing41, while shortened 1.0 d, 2.3 d, 5.0 d in Wuxiangjing14, respectively, as compared with that under T1D2. Under a certain temperature level at anthesis, the GD_{AM} decreased greatly with the increasing duration of high temperature, especially at T4 temperature level. Similar variations were found under the treatments from 12 days after anthesis (during grain-filling stage), but the shortened GD_{AM} in each combination of high temperature levels and high temperature durations at 12 days after anthesis were clearly smaller than that at anthesis. These results indicated that there was a great difference of heat sensitivity for GD_{AM} at different development stages, which means that the GD_{AM} was more affected by heat events closer to anthesis than those near maturity.

Significant positive relationship was found between the shortened GD_{AM} and heat degree-days (HDD) under post-anthesis heat stress (Fig. 3). With an increase of 1 °C d in HDD, the GD_{AM} under different treatments during anthesis reduced 0.64 d and 0.54 d, while 0.43 d and 0.34 d under the treatments from 12 days after anthesis (during grain-filling stage) in Nanjing41 and Wuxiangjing14, respectively. Overall, the acceleration of phenological process in Nanjing41 under post-anthesis heat stress was greater than that in Wuxiangjing14, which indicated that there were sensitivity differences in phenology response to heat stress among rice cultivars.

3.2. *Results of model calibration and genetic parameter estimation*

Two and three specific genetic parameters were used for predicting the main phenological stages of different rice cultivars in the original and improved models, respectively (Table 3). BFF was most related to different types of rice cultivars, and the value for indica rice is closer to 1 than that for japonica rice due to the shorter grain-filling duration in indica rice. From our samples, TS ranged from 2.2 to 4.8 among different cultivars. Overall, the best-fitted values of TS and BFF changed little between the original and improved models (Table 3). For the newly added parameter β in the improved model, greater values were found in japonica rice (0.21–0.80) than that in indica rice (0.06–0.20), which suggested that the japonica cultivar has higher heat sensitivity after anthesis compared with the indica cultivar.

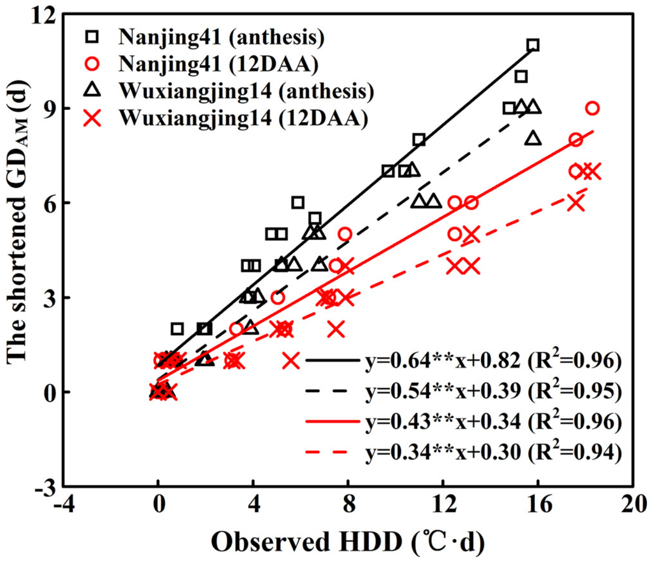

Fig. 3. Relationship between the shortened growing days from anthesis to maturity (GD_{AM}) and the post-anthesis heat degree-days (HDD) under different temperature treatments in phytotron in 2011–2013. 12DAA indicates temperature treatment at 12 days after anthesis.

Statistical analysis on the calibration results of RiceGrow model was shown in Table 4. Generally, there was a good agreement between the predicted and observed GD_{AM} under different temperature environments in RiceGrow, with RMSE of GD_{AM} less than 5 d for the original model while 3 d for the improved model. The average RMSE and S_d^2 of GD_{AM} in the improved model decreased 1.81 d and 6.04, respectively, as compared with that in the original model. Modeling efficiency greatly increased in the improved model as indicated by IA. Generally, both the original and improved models could achieve unbiased results between simulated and observed values according to MBE in Table 4 and the comparison results in Fig. S2.

3.3. *Model responses to simulated heat stresses at different days after anthesis*

Sensitivity analysis for GD_{AM} in response to the simulated heat stress occurred at different days after anthesis was carried out in the improved RiceGrow model. The result indicated that the GD_{AM} was more affected by heat stress near anthesis than those closer to maturity at different temperature regimes (Fig. 4). Heat stress with simulated temperature level of 41/31 °C shortened the GD_{AM} more obviously than that of 38/28 °C in the same phenological period. For example, the GD_{AM} was observed 45 d and 49 d under 41/31 °C and 38/28 °C, respectively, when heat stress applied from 1 d to 4 d after

Table 3
Genetic parameters for predicting physiological maturity.

Cultivar	Cropping season	Type and maturity	Original RiceGrow		Improved RiceGrow		
			TS	BFF	TS	BFF	β
Nanjing41	SR	Japonica and late	3.7	0.78	3.8	0.74	0.80
Wuxiangjing14	SR	Japonica and early	4.3	0.79	4.2	0.78	0.46
Wuyujing3	SR	Japonica and late	4.8	0.84	4.8	0.85	0.20
8304	SR	Japonica and mid	2.5	0.86	2.2	0.83	0.26
Shanyou63	SR	Indica and late	2.3	0.88	2.4	0.89	0.10
Xiang'aizao4	DER	Indica and late	3.1	0.97	3.3	0.96	0.05
Zhefu802	DER	Indica and early	2.9	0.95	3.2	0.95	0.18
Youl402	DER	Indica and early	2.8	0.93	3.0	0.97	0.06
73-07	DER	Indica and mid	2.6	0.94	2.8	0.93	0.17
Guanglu'ai4	DER	Indica and late	2.7	0.96	2.7	0.93	0.15

SR and DER indicate single-season rice and double-season early rice, respectively. TS: thermal sensitivity; BFF: basic filling factor; β: heat sensitivity factor.

Table 4
Calibration results of RiceGrow model on the growing days from anthesis to maturity (GD_{AM}) in different cultivars. Statistical indicators include root mean square error (RMSE), mean bias error (MBE), variance of the distribution of differences (S_d^2) and index of agreement (IA).

Cultivar	Original RiceGrow				Improved RiceGrow			
	RMSE	MBE	S_d^2	IA	RMSE	MBE	S_d^2	IA
Nanjing41	4.61	1.62	7.83	0.56	1.12	0.82	2.34	0.86
Wuxiangjing14	4.34	−0.96	6.14	0.61	0.96	−0.41	1.25	0.92
Wuyujing3	4.46	−0.30	11.87	0.80	2.44	0.90	1.50	0.78
8304	4.09	0.10	14.70	0.68	2.99	0.30	5.20	0.90
Shanyou63	4.13	−0.70	6.90	0.81	2.26	−0.50	5.10	0.87
Xiang'aizao4	2.86	−0.90	5.92	0.60	2.02	0.10	1.46	0.74
Zhefu802	4.05	1.20	16.04	0.48	2.16	−0.40	6.72	0.84
Youl402	2.90	−0.52	13.16	0.45	1.18	−0.80	6.61	0.57
73-07	2.72	2.70	7.74	0.51	1.76	0.90	3.23	0.79
Guanglu'ai4	2.50	1.40	6.91	0.77	1.67	−0.50	2.94	0.94
Average value	3.67	0.36	9.72	0.63	1.86	0.04	3.64	0.82

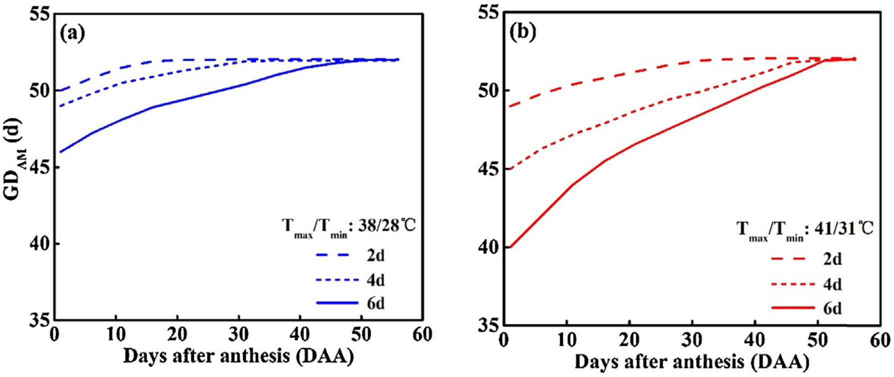

Fig. 4. Sensitivity analysis on the growing days from anthesis to maturity (GD_{AM}) in response to simulated heat events occurred at different days after anthesis (DAA). *In the simulated post-anthesis heat stress, two high-temperature levels (T_{max}/T_{min}) of 38/28 °C and 41/31 °C with three high-temperature durations (2 d, 4 d and 6 d) were applied starting from each available days after anthesis. In addition, the fixed daily temperature with T_{max}/T_{min} of 28/18 °C was used during the days after anthesis without heat events.

anthesis. At the same simulated temperature level, GD_{AM} decreased with increasing durations of heat stress after anthesis. These results suggested that the response to heat stress of phenology module in the improved RiceGrow was consistent with the experimental observation under high-temperature treatment at different post-anthesis development stage (Figs. 2 and 3).

3.4. Model validation

Fig. 5 showed that the prediction accuracy of the improved RiceGrow on phenological process under post-anthesis heat stress increased greatly as compared with the original RiceGrow. Given that the inherent simulation error was a constant, the difference of R^2 between the original and improved models approximately represented the difference of simulation precision under heat stress. In general, the simulation precision of phenology under post-anthesis heat stress increased 25% in the improved model (93.5% on average), as compared with the simulation precision in the original model (68.5% on average). In addition, a higher increasing rate of simulation precision was observed under phytotron environments (28%) than that under field conditions (22%).

A detailed comparison of validation results for the predicted GD_{AM} was shown in Table 5. The statistical analysis of validation results for different cultivars indicated that the performance on the estimation of phenology under post-anthesis heat stress was better in the improved model, with lower RMSE and S_d^2 than those in the original model. The average values of RMSE, MBE and S_d^2 for the predicted GD_{AM} decreased from 4.60 d, 2.65 d and 7.80 in the original model to 1.58 d, −0.16 d and 2.40, respectively, in the improved model under different post-anthesis heat stress environments. IA in the improved model increased 0.21 averagely. Simulation errors in the improved model under phytotron environments were generally smaller than that under field conditions, which was confirmed by the statistical indices of RMSE, MBE and S_d^2. In addition, the effects of model improvement would enhance with increasing heat degree-days (HDD). These results suggested that the prediction deviation for GD_{AM} in RiceGrow model might be enlarged with increasing temperature levels and temperature durations under post-anthesis heat stress.

Significant positive correlation ($p < 0.01$) between HDD and the prediction errors of GD_{AM} was observed in the original RiceGrow (Fig. 6), indicating that there were systematic errors in the estimation of phenological process for the original RiceGrow model under post-anthesis heat stress. The prediction error of GD_{AM} increased 0.44 d and 0.49 d with an increase of 1 °C d in HDD under phytotron and field conditions, respectively. For the improved model, the most systematic errors from the effect of post-anthesis heat stress were eliminated because there was no significant correlation between HDD and the prediction errors of GD_{AM}.

4. Discussion

4.1. Duration between anthesis and physiological maturity under post-anthesis heat stress

High temperature during reproductive stage has significantly accelerated the developmental process of crops, which probably becomes a main limiting factor to crop production because of the increasing occurrence of heat stress events (Battisti and Naylor, 2009; Gouache et al., 2012; Moriondo et al., 2011). Our study

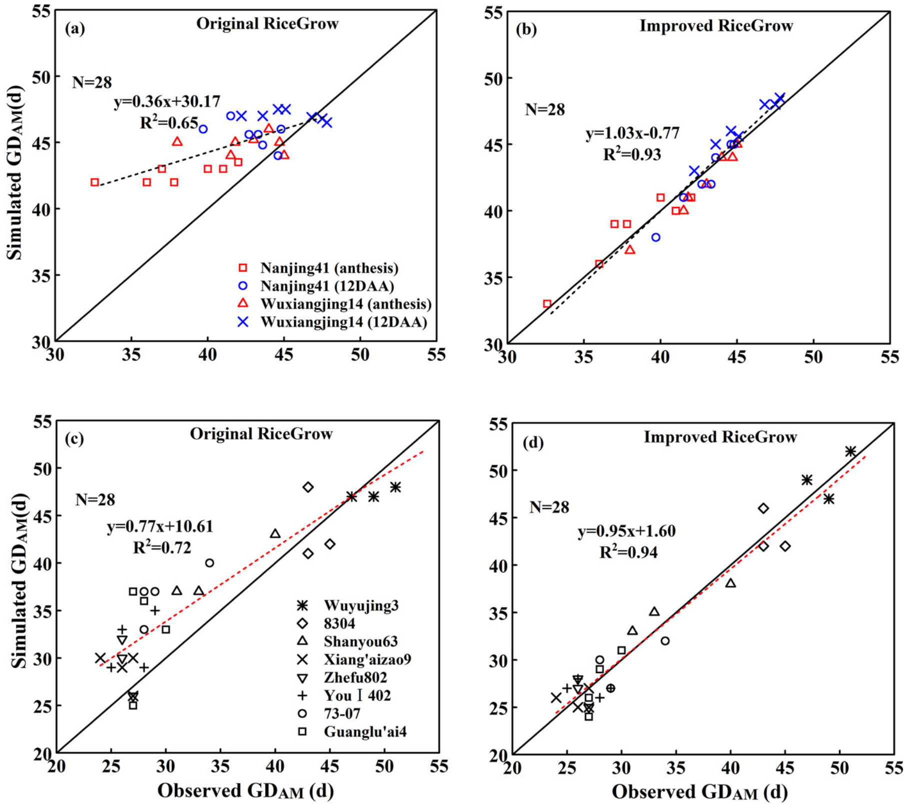

Fig. 5. Comparison of validation results between the observed and simulated growing days from anthesis to maturity (GD_{AM}) under different high temperatures in (a and b) phytotron and (c and b) field conditions. 12DAA indicates temperature treatment at 12 days after anthesis.

Table 5
Validation results of RiceGrow model on the growing days from anthesis to maturity (GD_{AM}) under different environments. Statistical indicators include root mean square error (RMSE), mean bias error (MBE), variance of the distribution of differences (S_d^2) and index of agreement (IA).

Experimental environment	Treatment	*N*	Original RiceGrow				Improved RiceGrow			
			RMSE	MBE	S_d^2	IA	RMSE	MBE	S_d^2	IA
Phytotron	T2 and T3 and T4	28	4.24	2.10	5.74	0.74	1.25	−0.12	2.03	0.90
	T2	4	2.42	−0.43	2.43	0.90	2.13	0.22	2.31	0.92
	T3	12	3.56	1.20	4.89	0.81	1.67	0.64	2.12	0.93
	T4	12	4.87	2.50	6.52	0.56	1.32	−0.25	1.46	0.91
Field	MHS and SHS	28	4.96	3.20	9.86	0.68	1.91	−0.20	2.77	0.94
	MHS	14	2.89	−0.12	6.68	0.87	1.98	−0.63	3.78	0.96
	SHS	14	6.53	5.10	7.07	0.54	1.83	0.65	2.65	0.88
Average value		28	4.60	2.65	7.80	0.71	1.58	−0.16	2.40	0.92

MHS and SHS indicate phenological data from the years with moderate heat stress (HDD < 10 °C) and severe heat stress (HDD ≥ 10 °C) from anthesis to maturity under field conditions, respectively.

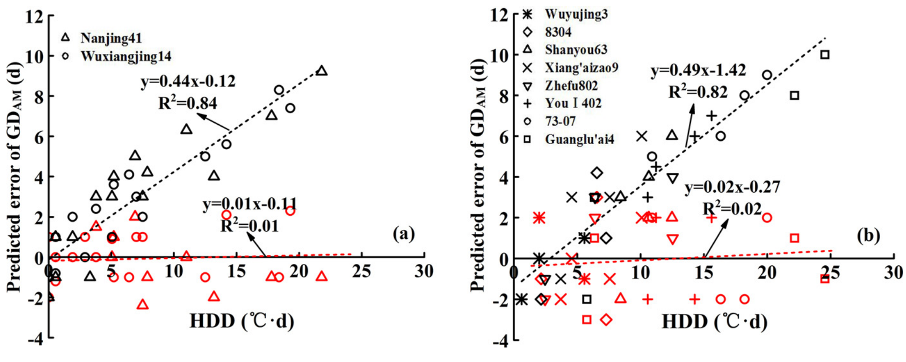

Fig. 6. Correlations between the prediction errors of the growing days from anthesis to maturity (GD_{AM}) and the observed heat degree-days (HDD) under (a) phytotron and (b) field conditions. Black and red symbols indicate the validation results of the original and improved RiceGrow models, respectively. (For interpretation of the references to color in this figure legend, the reader is referred to the web version of this article.)

found a significant decline in grain filling duration and an obvious advance in physiological maturity for japonica rice under post-anthesis heat stress (Figs. 2 and 3). The acceleration of grain filling process under high temperature stress was confirmed by many previous studies, yet few reports mentioned the determination of physiological maturity. Usually, physiological maturity in rice can be determined by leaf senescence, grain color and grain weight. Under normal environment, these traits almost characterize physiological maturity at the same time, i.e. about half leaves in a plant turn yellow, more than 95% grains in a panicle have yellow husks and all filled grains attain to maximum dry weight. However, when rice suffers severe heat stress during reproductive stage, these traits cannot reach the specific physiological status at physiological maturity simultaneously. High temperature at reproductive stage often causes poor pollination and fertilization, which will lead to a great loss of sink activity. In such situations, the translocation of assimilates from leaves to grains will be limited and the leaf senescence will be delayed. In addition, sterile grains in panicles always stay green before harvest, while the fertilized grains turn yellow in the process of ripening (Fig. S3). Similar phenomena were observed in previous studies (Kim et al., 2011; Nakano et al., 1995; Prasad et al., 2008). Therefore, the measurement of physiological maturity according to grain color or leaf senescence is not feasible, especially when rice suffers heat events during reproductive stage. In contrast, grain weight is the most concerned indicator at harvest time and is able to reach the maximum value at physiological maturity. The measurement of physiological maturity on the basis of grain weight can reflect the ripening process of rice crop more accurately under high temperature environment.

4.2. Simulation of phenological response under heat stress

The phenology response of crop models to climate warming has attracted increasing attentions in recent years, especially under heat stress conditions. Previous studies have noticed the poor predictions and systematic errors for current phenology models under heat stress conditions (Alderman et al., 2013; Van Oort et al., 2011; Zhang et al., 2008). Researchers put more emphasis on the better calibration for phenological parameters under heat stress, while relatively little work has been done on simulating the response of crop phenology to heat stress. Van Oort et al. (2011) emphasized that more phenological studies in rice will be needed for the average growing season temperature above the optimum. Our study improved the phenology response to high temperature within the daily maximal temperature range of 35–41 °C. Phenology simulation in the improved model was not only depended on the effect of normal temperature but also on the effect of heat stress. Thermal effectiveness of the improved model was consisted of two parts: thermal effectiveness of normal temperature, which was similar as the assumption in most phenology model; and an additional response to the high temperature, i.e. thermal effectiveness of heat stress, which reflected the acceleration for the phenological development under heat stress.

Among the existing models, CERES-Rice, ORYZA2000, GECROS, RCM and Beta Model predict the delay in development rate above the optimum temperature (T_o), while SIMRIW model predicts that the development rate remains constant for temperatures above the T_o (Van Oort et al., 2011; Yin and van Laar, 2005; Zhang and Tao, 2013). In summary, phenology responses of most crop models show either constant or decreasing development rate to high temperature above the optimum. In contrast, our study reports an increasing development rate above the threshold temperature of heat stress ($T_h = 35\,^{\circ}\mathrm{C}$) after anthesis in the improved RiceGrow model, which gave better prediction than the original model with a constant development rate above the threshold temperature of heat stress. In addition, the sensitivity analysis indicated that the duration of grain filling was more affected by heat events closer to anthesis than those near maturity in the improved model, which was consistent with the previous report on heat stress (Asseng et al., 2011).

4.3. High-temperature experiments under controlled environments

High-temperature experiments under controlled environments are becoming more important in estimating crop responses to climate change (White et al., 2011; Wolkovich et al., 2012). It is difficult to quantify the effects of heat stress on crop growth under field conditions because of the uncontrollable environment. The environment-controlled experiments provide a powerful adjunct to the study on climatic effects (Robertson et al., 1998). In some previous studies, many facilities in environmentally controlled chambers employed a square-wave temperature regime for the diurnal variation of temperature, with temperature differences in a day only between daytime and nighttime (Cheng et al., 2010; Mohammed and Tarpley, 2009). This temperature change pattern was not consistent with temperature variation in natural systems, and might confound experimental data due to the different crop responses to different daily temperature variation (Wolkovich et al., 2012). In contrast, temperature gradient chambers (TGCs) allowed the study of temperature effects on crops under field-like conditions and the temperatures inside could generally keep track with the ambient temperatures (Horie et al., 1995; Rawson et al., 1995). Based on the design concepts of TGCs, our phytotron was equipped with temperature system that could simulate natural diurnal temperature variation with different amplitudes in a day (Fig. 1). Observed phenological data under heat stress with daily temperature variation in this control mode would be more consistent to the real response of rice growth to high temperature in natural systems. Wolkovich et al. (2012) suggesed that the reliability of experimental data derived from the controlled environment should be verified under field conditions. In our study, the improved model developed with phenological data from temperature-controlled experiments was calibrated and validated with phenological data from different cultivars under field conditions at different locations. Results showed that simulation errors for the improved model under phytotron and field environments were generally similar (Tables 4 and 5). Hence, the improved model developed with phenological data in phytotron can be applied to field conditions.

4.4. The argues and shortcomings

Previous studies showed that the developmental process and duration of grain filling were affected both by the supply of assimilate source, i.e. leaf and stem, and by the sink activity of reproductive organ, i.e. spikelets in panicle (Kim et al., 2011; Krishnan et al., 2011; Prasad et al., 2008). The critical high temperature in vegetative organs was ususlly considered slightly higher than reproductive organs (Luo, 2011; Prasad et al., 2008). Sanchez et al. (2014) reported that 35.4 °C was the critical high temperature for the whole plant in rice. Many studies considered 35 °C as the critical high temperature for spikelet fertility during reproductive stage (Huo and Wang, 2009; Luo, 2011; Wassmann et al., 2009). Theoretically, the threshold temperature of heat stress (T_h) varys with different organs, cultivars and developmental stages in rice. However, a fixed threshold temperature of heat stress is important for the determination of genetic parameters in crop model, because it can effectively decrease the number of parameters and improve the efficiency of model simulation. In our phytotron experiment, no obvious reduction of GD_{AM} under T2 treatment (35/25 °C) with 2 days duration was observed, while obvious reduction of GD_{AM}

under T2 treatment (35/25 °C) with 6 days duration was observed, as compared with that under T1 treatment (32/22 °C) (Fig. 2). Thus, by comprehensively analyzing our experiment results in phytotron and previous reports in rice (Sun and Huang, 2011; Teixeira et al., 2013; Yu et al., 2010), T_h after anthesis was set as 35 °C in the improved model. However, more precise estimation of T_h in rice crop is needed in the future.

Since the ceiling temperature for rice growth is not clear according to current experimental treatments, there is an important uncertainty of phenology simulation in RiceGrow model under the temperatures above 41 °C (the highest temperature level in our temperature-controlled experiments). In addition, the development rate from the optimum temperature ($T_o = 30$ °C) to the threshold temperature of heat stress ($T_h = 35$ °C) still kept constant in the improved RiceGrow. In order to simplify the simulation of development rate, a continuous increase of development rate from the base temperature (T_b) to T_h was hypothesized by setting the optimum temperature (T_o) to 35 °C. However, significant increase ($p < 0.05$) of prediction error was found for the hypothesized model (Tables 4 and S1). This suggested that a constant development rate between T_o and T_h might be more suitable to reflect phenology response to temperature based on current dataset although the physiological mechanism was not clear. Therefore further studies will focus on the determination of lethal temperature and the deeper understanding of phenology response to heat stress in rice.

5. Conclusions

Post-anthesis heat stress shortened the duration of grain filling in rice, which resulted in early physiological maturity. Significant positive relationship was observed between the grain growing days from anthesis to maturity (GD_{AM}) and heat degree-days (HDD). Based on the response of rice phenology to high temperatures, the thermal effectiveness caused by heat stress was supplemented to RiceGrow model. Model performance on phenological process in response to post-anthesis heat stress was tested under both phytotron and field conditions. The improved RiceGrow model had a better performance on different cultivars and heat events occurred at different development stages after anthesis, with a 25% increase in simulation precision for GD_{AM}, as compared with the original model under post-anthesis heat stress. Our study proposed a novel approach to estimate the probable effect of extreme high temperature on rice phenology by quantifying the heat-induced thermal effectiveness. More studies on the response of phenological process to heat stress are helpful for the improvement of global crop models under climate change.

Acknowledgments

This work was supported by the National High-Tech Research and Development Program of China (2013AA100404, 2012AA101906-1) and the Priority Academic Program Development of Jiangsu Higher Education Institutions (PAPD). We gratefully acknowledge the kind help from Bing Liu in the writing of R program.

Appendix A. Supplementary data

Supplementary data associated with this article can be found, in the online version, at http://dx.doi.org/10.1016/j.fcr.2015.02.023.

References

Alderman, P.D., Quilligan, E., Asseng, S., Ewert, F., Reynolds, M.P., 2013. Proceedings of the Workshop on Modeling Wheat Response to High Temperature. International Maize and Wheat Improvement Center, Mexico.

Angulo, C., Rötter, R., Lock, R., Enders, A., Fronzek, S., Ewert, F., 2013. Implication of crop model calibration strategies for assessing regional impacts of climate change in Europe. Agric. For. Meteorol. 170, 32–46.

Asseng, S., Foster, I., Turner, N., 2011. The impact of temperature variability on wheat yields. Global Change Biol. 17, 997–1012.

Battisti, D.S., Naylor, R.L., 2009. Historical warnings of future food insecurity with unprecedented seasonal heat. Science 323, 240–244.

Boote, K.J., Jones, J.W., Pickering, N.B., 1996. Potential uses and limitations of crop models. Agron. J. 88, 704–716.

Bouman, B., 2001. ORYZA2000: Modeling Lowland Rice. International Rice Research Institute/Wageningen University and Research Centre, Los Baños, Philippines/Wageningen, Netherlands.

Cao, W., Moss, D., 1997. Modelling phasic development in wheat: a conceptual integration of physiological components. J. Agric. Sci. 129, 163–172.

Casa, R., Varella, H., Buis, S., Guérif, M., De Solan, B., Baret, F., 2012. Forcing a wheat crop model with LAI data to access agronomic variables: evaluation of the impact of model and LAI uncertainties and comparison with an empirical approach. Eur. J. Agron. 37, 1–10.

Cheng, W., Sakai, H., Yagi, K., Hasegawa, T., 2010. Combined effects of elevated CO_2 and high night temperature on carbon assimilation, nitrogen absorption, and the allocations of C and N by rice (*Oryza sativa* L.). Agric. For. Meteorol. 150, 1174–1181.

Chmielewski, F.M., Müller, A., Bruns, E., 2004. Climate changes and trends in phenology of fruit trees and field crops in Germany, 1961–2000. Agric. For. Meteorol. 121, 69–78.

Gouache, D., Le Bris, X., Bogard, M., Deudon, O., Pagé, C., Gate, P., 2012. Evaluating agronomic adaptation options to increasing heat stress under climate change during wheat grain filling in France. Eur. J. Agron. 39, 62–70.

Hanft, J.M., Wych, R.D., 1982. Visual indicators of physiological maturity of hard red spring wheat. Crop Sci. 22, 584–588.

Horie, T., Nakagawa, H., Nakano, J., Hamotani, K., Kim, H., 1995. Temperature gradient chambers for research on global environment change. III. A system designed for rice in Kyoto, Japan. Plant Cell Environ. 18, 1064–1069.

Huo, Z., Wang, S., 2009. Agricultural and Biometeorological Disasters. China Meteorological Press, Beijing, China (in Chinese).

Jégo, G., Pattey, E., Liu, J., 2012. Using Leaf Area Index, retrieved from optical imagery, in the STICS crop model for predicting yield and biomass of field crops. Field Crops Res. 131, 63–74.

Jones, D., Peterson, M., Geng, S., 1979. Association between grain filling rate and duration and yield components in rice. Crop Sci. 19, 641–644.

Kim, J., Shon, J., Lee, C., Yong, Y., Yang, W., Kim, Y., Lee, B., 2011. Relationship between grain filling duration and leaf senescence of temperate rice under high temperature. Field Crops Res. 122, 207–213.

Krishnan, P., Ramakrishnan, B., Reddy, K.R., Reddy, V., 2011. High temperature effects on rice growth, yield, and grain quality. Adv. Agron. 111, 87–206.

Liu, L., Wang, E., Zhu, Y., Tang, L., 2012. Contrasting effects of warming and autonomous breeding on single-rice productivity in China. Agric. Ecosyst. Environ. 149, 20–29.

Liu, L., Wang, E., Zhu, Y., Tang, L., Cao, W., 2013. Effects of warming and autonomous breeding on the phenological development and grain yield of double-rice systems in China. Agric. Ecosyst. Environ. 165, 28–38.

Lloret, F., Escudero, A., Iriondo, J.M., Martínez-Vilalta, J., Valladares, F., 2012. Extreme climatic events and vegetation: the role of stabilizing processes. Global Change Biol. 18, 797–805.

Lobell, D.B., Bänziger, M., Magorokosho, C., Vivek, B., 2011. Nonlinear heat effects on African maize as evidenced by historical yield trials. Nat. Clim. Change 1, 42–45.

Lobell, D.B., Hammer, G.L., McLean, G., Messina, C., Roberts, M.J., Schlenker, W., 2013. The critical role of extreme heat for maize production in the United States. Nat. Clim. Change 3, 497–501.

Lobell, D.B., Sibley, A., Ortiz-Monasterio, J.I., 2012. Extreme heat effects on wheat senescence in India. Nat. Clim. Change 2, 186–189.

Luo, Q., 2011. Temperature thresholds and crop production: a review. Clim. Change 109, 583–598.

McMaster, G.S., White, J.W., Hunt, L., Jamieson, P., Dhillon, S., Ortiz-Monasterio, J., 2008. Simulating the influence of vernalization, photoperiod and optimum temperature on wheat developmental rates. Ann. Bot. 102, 561–569.

Meng, Y., Cao, W., Zhou, Z., Liu, X., 2003. A process-based model for simulating phasic development and phenology in rice. Agric. Sci. China 2, 1277–1284.

Mohammed, A.R., Tarpley, L., 2009. Impact of high nighttime temperature on respiration, membrane stability, antioxidant capacity, and yield of rice plants. Crop Sci. 49, 313–322.

Moriondo, M., Giannakopoulos, C., Bindi, M., 2011. Climate change impact assessment: the role of climate extremes in crop yield simulation. Clim. Change 104, 679–701.

Nakano, H., Makino, A., Mae, T., 1995. Effects of panicle removal on the photosynthetic characteristics of the flag leaf of rice plants during the ripening stage. Plant Cell Physiol. 36, 653–659.

Nelder, J.A., Mead, R., 1965. A simplex method for function minimization. Comput. J. 7, 308–313.

Van Oort, P.A.J., Zhang, T., Vries, M.E., Heinemann, A.B., Meinke, H., 2011. Correlation between temperature and phenology prediction error in rice (*Oryza sativa* L.). Agric. For. Meteorol. 151, 1545–1555.

Palosuo, T., Kersebaum, K.C., Angulo, C., Hlavinka, P., Moriondo, M., Olesen, J.E., Patil, R.H., Ruget, F., Rumbaur, C., Takáč, J., Trnka, M., Bindi, M., Çaldağ, B., Ewert, F., Ferrise, R., Mirschel, W., Şaylan, L., Šiška, B., Rötter, R., 2011. Simulation of winter wheat yield and its variability in different climates of Europe: a comparison of eight crop growth models. Eur. J. Agron. 35, 103–114.

Prasad, P.V.V., Boote, K., Allen Jr., L., Sheehy, J., Thomas, J., 2006. Species, ecotype and cultivar differences in spikelet fertility and harvest index of rice in response to high temperature stress. Field Crops Res. 95, 398–411.

Prasad, P.V.V., Staggenborg, S.A., Ristic, Z., 2008. Impacts of Drought and/or Heat Stress on Physiological, Developmental, Growth, and Yield Processes of Crop Plants. Response of Crops to Limited Water: Understanding and Modeling Water Stress Effects on Plant Growth Processes. ASA, CSSA, SSSA, Madison, WI, USA, pp. 301–355.

R Core Team, 2014. R: A Language and Environment for Statistical Computing. R Foundation for Statistical Computing, Vienna, Austria http://www.R-project.org/

Rötter, R.P., Palosuo, T., Kersebaum, K.C., Angulo, C., Bindi, M., Ewert, F., Ferrise, R., Hlavinka, P., Moriondo, M., Nendel, C., Olesen, J.E., Patil, R.H., Ruget, F., Takáč, J., Trnka, M., 2012. Simulation of spring barley yield in different climatic zones of Northern and Central Europe: a comparison of nine crop models. Field Crops Res. 133, 23–36.

Rawson, H., Gifford, R., Condon, B., 1995. Temperature gradient chambers for research on global environment change. I. Portable chambers for research on short-stature vegetation. Plant Cell Environ. 18, 1048–1054.

Robertson, M.J., Bonnett, G.D., Hughes, R.M., Muchow, R.C., Campbell, J.A., 1998. Temperature and leaf area expansion of sugarcane: integration of controlled-environment, field and model studies. Aust. J. Plant Physiol. 25, 819–828.

Sadras, V.O., Monzon, J.P., 2006. Modelled wheat phenology captures rising temperature trends: shortened time to flowering and maturity in Australia and Argentina. Field Crops Res. 99, 136–146.

Sanchez, B., Rasmussen, A., Porter, J.R., 2014. Temperatures and the growth and development of maize and rice: a review. Global Change Biol. 20, 408–417.

Schlenker, W., Roberts, M.J., 2009. Nonlinear temperature effects indicate severe damages to US crop yields under climate change. PNAS 106, 15594–15598.

Shaw, R.H., Loomis, W.E., 1950. Bases for the prediction of corn yields. Plant Physiol. 25, 225–244.

Sun, W., Huang, Y., 2011. Global warming over the period 1961–2008 did not increase high-temperature stress but did reduce low-temperature stress in irrigated rice across China. Agric. For. Meteorol. 151, 1193–1201.

Tang, L., Zhu, Y., Hannaway, D., Meng, Y., Liu, L., Chen, L., Cao, W., 2009. RiceGrow: a rice growth and productivity model. NJAS-Wagen. J. Life Sci. 57, 83–92.

Tao, F., Yokozawa, M., Xu, Y., Hayashi, Y., Zhang, Z., 2006. Climate changes and trends in phenology and yields of field crops in China, 1981–2000. Agric. For. Meteorol. 138, 82–92.

Teixeira, E.I., Fischer, G., van Velthuizen, H., Walter, C., Ewert, F., 2013. Global hot-spots of heat stress on agricultural crops due to climate change. Agric. For. Meteorol. 170, 206–215.

Wallach, D., 2011. Crop model calibration: a statistical perspective. Agron. J. 103, 1144–1151.

Wassmann, R., Jagadish, S., Heuer, S., Ismail, A., Redona, E., Serraj, R., Singh, R., Howell, G., Pathak, H., Sumfleth, K., 2009. Climate change affecting rice production: the physiological and agronomic basis for possible adaptation strategies. Adv. Agron. 101, 59–122.

White, J.W., Hoogenboom, G., 2010. Crop response to climate: ecophysiological models. In: Climate Change and Food Security. Springer, The Netherlands, pp. 59–83.

White, J.W., Kimball, B.A., Wall, G.W., Ottman, M.J., Hunt, L., 2011. Responses of time of anthesis and maturity to sowing dates and infrared warming in spring wheat. Field Crops Res. 124, 213–222.

White, M.A., Thornton, P.E., Running, S.W., 1997. A continental phenology model for monitoring vegetation responses to interannual climatic variability. Global Biogeochem. Cycles 11, 217–234.

Wolkovich, E.M., Cook, B.I., Allen, J.M., Crimmins, T.M., Betancourt, J.L., Travers, S.E., Pau, S., Regetz, J., Davies, T.J., Kraft, N.J., Ault, T.R., Bolmgren, K., Mazer, S.J., McCabe, G.J., McGill, B.J., Parmesan, C., Salamin, N., Schwartz, M.D., Cleland, E.E., 2012. Warming experiments underpredict plant phenological responses to climate change. Nature 485, 494–497.

Xue, Q., Weiss, A., Baenziger, P.S., 2004. Predicting phenological development in winter wheat. Clim. Res. 25, 243–252.

Yin, X., van Laar, H.H., 2005. Crop Systems Dynamics: An Ecophysiological Simulation Model for Genotype-by-Environment Interactions. Wageningen Academic Publisher, Wageningen, pp. 40–42.

Yu, K., Song, J., Gao, P., 2010. Characteristics of heat damage for rice in Jiangsu province. Sci. Meteorol. Sin. 30, 530–533 (in Chinese with English abstract).

Zhang, S., Tao, F., 2013. Modeling the response of rice phenology to climate change and variability in different climatic zones: comparisons of five models. Eur. J. Agron. 45, 165–176.

Zhang, T., Zhu, J., Yang, X., 2008. Non-stationary thermal time accumulation reduces the predictability of climate change effects on agriculture. Agric. For. Meteorol. 148, 1412–1418.

Zhang, X., Meinke, H., DeVoil, P., van Laar, H.H., Bouman, B.A.M., Abawi, Y., 2004. Simulating growth and development of lowland rice in APSIM. In: Proceedings of the 4th International Crop Science Congress, Brisbane, Australia, p. 333-333.

Zhu, Q., Cao, X., Luo, Y., 1988. Growth analysis on the process of grain filling in rice. Acta Agron. Sin. 14, 182–193 (in Chinese with English abstract).